

UC Berkeley

UC Berkeley Previously Published Works

Title

Transcranial Magnetic Stimulation Changes Response Selectivity of Neurons in the Visual Cortex

Permalink

<https://escholarship.org/uc/item/0xj6b6rd>

Journal

Brain Stimulation, 8(3)

ISSN

1935-861X

Authors

Kim, Taekjun
Allen, Elena A
Pasley, Brian N
[et al.](#)

Publication Date

2015-05-01

DOI

10.1016/j.brs.2015.01.407

Peer reviewed



Published in final edited form as:

Brain Stimul. 2015 ; 8(3): 613–623. doi:10.1016/j.brs.2015.01.407.

Transcranial magnetic stimulation changes response selectivity of neurons in the visual cortex

Taekjun Kim¹, Elena A. Allen², Brian N. Pasley², and Ralph D. Freeman^{1,2}

¹Vision Science Graduate Group, University of California, Berkeley, CA 94720

²Helen Wills Neuroscience Institute, and School of Optometry, University of California, Berkeley, CA 94720

Abstract

Background—Transcranial magnetic stimulation (TMS) is used to selectively alter neuronal activity of specific regions in the cerebral cortex. TMS is reported to induce either transient disruption or enhancement of different neural functions. However, its effects on tuning properties of sensory neurons have not been studied quantitatively.

Objective/Hypothesis—Here, we use specific TMS application parameters to determine how they may alter tuning characteristics (orientation, spatial frequency, and contrast sensitivity) of single neurons in the cat's visual cortex.

Methods—Single unit spikes were recorded with tungsten microelectrodes from the visual cortex of anesthetized and paralyzed cats (12 males). Repetitive TMS (4Hz, 4sec) was delivered with a 70mm figure-8 coil. We quantified basic tuning parameters of individual neurons for each pre- and post-TMS condition. The statistical significance of changes for each tuning parameter between the two conditions was evaluated with a Wilcoxon signed-rank test.

Results—We generally find long-lasting suppression which persists well beyond the stimulation period. Pre- and post-TMS orientation tuning curves show constant peak values. However, strong suppression at non-preferred orientations tends to narrow the widths of tuning curves. Spatial frequency tuning exhibits an asymmetric change in overall shape, which results in an emphasis on higher frequencies. Contrast tuning curves show nonlinear changes consistent with a gain control mechanism.

© 2015 Elsevier Inc. All rights reserved.

Corresponding author: Ralph D. Freeman, 360 Minor Hall, UC Berkeley School of Optometry, Berkeley, CA 94720, rfreeman@berkeley.edu.

Current address of Elena A. Allen is: The Mind Research Network, 1101 Yale Blvd. NE., Albuquerque, New Mexico 87106.

Publisher's Disclaimer: This is a PDF file of an unedited manuscript that has been accepted for publication. As a service to our customers we are providing this early version of the manuscript. The manuscript will undergo copyediting, typesetting, and review of the resulting proof before it is published in its final citable form. Please note that during the production process errors may be discovered which could affect the content, and all legal disclaimers that apply to the journal pertain.

Author contributions:

T.K., E.A.A., B.N.P., & R.D.F. contributed to conception and design of the experiments. T.K., E.A.A., & B.N.P. collected data. T.K. analyzed the data. T.K. and R.D.F. wrote the manuscript. T.K., E.A.A., B.N.P., & R.D.F. approved the final version.

Conflict of Interest:

The authors declare no competing financial interests.

Conclusions—These findings suggest that TMS causes extended interruption of the balance between sub-cortical and intra-cortical inputs.

Keywords

Transcranial magnetic stimulation; orientation, spatial frequency, contrast selectivity; single unit activity

Introduction

Historically, numerous attempts have been made to alter brain activity in normal and abnormal physiological conditions. A prominent approach has been used to modify function by use of external application of electrical fields [1–3]. In addition to attempts to alter normal function, approaches have been used to treat clinical disorders by use of electrical stimulation. A relatively noninvasive technique, transcranial magnetic stimulation (TMS), has been shown to modify motor function in the human brain [4,5]. This has led to numerous studies [6–8].

Although consequences of specific parameters of TMS have been studied, numerous factors complicate interpretation. Variables include: different brain regions and cell types, various synaptic mechanisms, input and output patterns to local areas of the brain, and stimulation parameters. Reported TMS neural findings include: facilitation or suppression or both in specific brain areas [9–12]. Variability is substantial within both normal and abnormal subject populations [13,14]. In addition, TMS effects may rely on initial cortical activation state or excitability levels of specific neural populations [15–17].

This background suggests the need for a focused procedure with limited parameters. The physiological parameters of visual cortical neurons are well established. In addition, we have previously studied these responses in relation to hemodynamic signals and state dependent characteristics following TMS application [17,18]. Here, we investigate how basic tuning properties of cortical cells are affected by repetitive TMS (rTMS).

Although TMS effects on neural selectivity have been addressed previously, [19–21], former work concerned neural selectivity at population levels. This involved causal relations between targeted brain areas and behavioral tasks. Our current study involves TMS effects on cortical response selectivity, quantified at a cellular level. Based on well-established knowledge of the central visual pathway, our findings provide clues for understanding neural mechanism of TMS effects.

Materials and Methods

Animal preparation

Single unit spikes and LFP data were collected from the visual cortex of anesthetized and paralyzed cats (12 males). All procedures were conducted in accordance with guidelines by NIH and by the Animal Care and Use Committee at the University of California, Berkeley. We induced initial anesthesia with 3% isoflurane, and inserted venous catheters for continuous infusion of drugs during surgery and recording. While a tracheotomy and a

craniotomy (Horsley-Clarke coordinates P4L2) were performed, anesthesia was maintained with continuous propofol (20mg/kg-hr) and fentanyl (10 μ g/kg-hr). After the surgery, infusion rates of continuous propofol (6~8mg/kg-hr) and fentanyl (4 μ g/kg-hr) were adjusted individually for each animal to be at an adequate level of anesthesia. Then, to prevent eye movements, the animal was paralyzed with continuous pancuronium (0.2mg/kg-hr).

Transcranial magnetic stimulation (TMS)

TMS was delivered with a 70mm figure-8 coil connected to a Magstim Rapid stimulator (Magstim Company, Whitland, UK). Electrode penetration was made at an angle of A45, M0 (Figure 1A). This allows the figure-8 coil to be positioned obliquely near the transverse plane superior to the visual cortex [17,18]. The midpoint of the coil was centered on the left visual cortex craniotomy, 1.5~2cm from the skull. TMS pulse trains (4Hz, 4sec) were delivered by a TTL digital pulse at 80~100% stimulation intensity. At this intensity and range of distances, the induced electric field strength is estimated to be ~100-160 V/m [22].

Recording procedure

Neural activity was recorded with two-channel tungsten microelectrodes. Amplified raw signals from each electrode were bifurcated and fed into a band-pass filter to extract spike (500Hz ~ 8MHz) and LFP (0.7~170Hz) activity. Single units were identified based on spike waveform. Time stamps of single unit spikes and digitized LFPs were saved at resolutions of 25kHz and 500Hz, respectively. Analysis methods and results from LFP data are available in Supplementary Materials.

Once a single unit was well isolated, several procedures were run to find the optimal drifting sinusoidal grating stimulus (50% contrast) that evokes the maximum response of the unit (orientation \rightarrow spatial frequency \rightarrow temporal frequency \rightarrow binocular phase (for binocular cell) \rightarrow size). And the obtained parameters were used to get detailed quantitative tuning properties for the main measurements.

To get detailed orientation tuning, we used 10 orientation values for each trial spanning 90 $^{\circ}$ with the pre-determined optimal orientation as the center (e.g., 0~90 $^{\circ}$ at intervals of 10 $^{\circ}$). The other parameters of drifting sinusoidal grating stimuli were fixed at optimal values. Both stimulus duration and inter-stimulus interval were set at 2 seconds, so a total of 40 seconds was required for all 10 tested orientations to be presented per trial. Short TMS pulse trains (4Hz, 4sec) were delivered just before the beginning of the 16th trial (Figure 1B). 15 trials before (trials 1~15) and after (trials 16~30) the TMS delivery were used to create two orientation tuning curves for the comparison between pre- and post-TMS conditions. Pre- and post-TMS trials corresponded to times of around -12.5~0 minutes and 0~12.5 minutes, respectively. Procedures to obtain spatial frequency and contrast tuning curves were identical to those for orientation. But the range of 10 tested values was fixed regardless of a cell's preference (Spatial frequency: 0.1~2 c/deg, Contrast: 5~100%; values were evenly distributed on a logarithmic scale). For some cells, fewer values (7~8) were tested to save time.

Data analysis

- Fitting of basic tuning curves

To quantify the effects of TMS on orientation tuning properties, individual tuning curves were fitted with a Gaussian function as follows.

$$R(x) = K \times \exp\left(\frac{-(x - \mu)^2}{2 \times \sigma^2}\right) + R_0 \quad (1)$$

where K is the maximum neural response, x is the orientation, μ is the preferred orientation, σ is the standard deviation of the Gaussian, and R_0 represents the baseline neural response when visual stimulation is not provided. The spatial frequency tuning curves were also fitted with the same function as above. But note that they are not Gaussian shaped when the x-axis is transformed to a logarithmic scale.

The contrast tuning curves were fitted using the Naka-Rushton function [23].

$$R(c) = \frac{R_{max} C^n}{C^n + C_{50}^n} + R_0 \quad (2)$$

where R_{max} is the asymptotic maximum neural response, c is the contrast, c_{50} is the contrast at which the fitted curve reaches half of the maximum, n is the power function exponent, and R_0 represents the baseline neural response when visual stimulation is not employed.

For individual neurons, tuning parameters were computed for each pre- and post-TMS condition. In order to understand the overall effects of TMS on functional tuning, the statistical significance of changes for each tuning parameter between two conditions was evaluated with a Wilcoxon signed-rank test.

Results

We studied 133 neurons from the visual cortices of 12 animals. We examined in detail effects of TMS on tuning properties of orientation, spatial frequency, and contrast sensitivity for 35, 32, and 25 cells, respectively (a total of 92 neurons). The excluded cells were either not affected by TMS due to poor positioning of the magnetic coil, lost during recording, or exhibited erratic behavior such as sudden neuronal silence or spike bursts independent of TMS application that prevented quantitative analysis.

TMS effects on orientation tuning: representative neurons

In previous initial studies, we used short TMS pulse trains and found, in most cases, that single unit neural activity in visual cortex was substantially suppressed for long periods [17,18]. Our current experiments yield similar findings. For this result in Figure 2A, the orientation of a grating has been varied between 40° and 130° in 10° steps presented in random order. Orientation is represented along the ordinate and response strength is color-coded according to the scale on the right. Neural activity is strongest in the red region and weakest in the blue. The abscissa shows trial number and time relative to application of TMS. At the top, a scale shows black filled circles followed by gray and then open which

represent, respectively, pre-TMS, post-TMS, and recovery conditions. The downward open arrow indicates when TMS has been applied. A relatively wide range of orientations, centered at the peak value of 80° , is active prior to application of TMS. During the first 15 trials prior to delivery of TMS, which corresponds to $-12.5\sim 0$ minutes, neural activity for all orientations tested is relatively stable. After TMS is delivered between the 15th and 16th trial (time = 0), there is a clearly diminished response over the range of tested orientations. Note for this case and in general, TMS induced suppression is sustained for several minutes or more after completion of a 4 seconds TMS application (see Time axis at the bottom of Figure 2A).

These results are shown graphically in Figure 2B. Maximum suppression occurs at 80° and responses are reduced on both sides of the peak over the entire responsive part of the tuning curve. Note that the change in neural activity is similar in shape but not in magnitude (black vs. gray line curve), for the preferred orientation (80°) and non-preferred (e.g., 100°). Also, recovery is not complete as the dashed line curve remains lower than that of the pre-TMS condition even at a recovery period of $12.5\sim 22.5$ minutes after TMS application.

Another example, presented in Figure 2C & D, shows an effect of TMS that is more severe than in the previous case. Substantial suppression occurs immediately following TMS delivery (downward open arrow). Note in Figure 2C and D, the very low response level during the period indicated by gray dots. The suppression lasted for 12.5 minutes. It is also clear in this case and many others that the lower response after TMS results in a narrowing of the tuning width. Although, again, the recovery brings the response level back to nearly that of pre-TMS delivery, the overall tuning curve response is still slightly lower (dashed line curve) at times of 12.5 to 22.5 minutes after TMS application. The final example of Figure 2 (E and F) is an exception to the general finding that our 4Hz rTMS nearly always results in prolonged suppression of neural responses (80 out of 92 units). For a small number of cases, as in this example, TMS caused facilitation instead of suppression. Note that the pre-TMS filled circles section of the response is considerably lower than that following application of TMS as illustrated by the gray line graph. Again, maximum facilitation occurs at the preferred orientation (110°) and effects tapering off on either side of optimal. Recovery data for this example (dashed line) shows that restoration remains relatively limited and clearly below that of the facilitation level even after periods of 12.5 to 22.5 minutes.

TMS effects on spatial frequency tuning: representative neurons

As in the case of orientation, spatial frequency is a central parameter of sinusoidal grating stimuli. Similar data to those for orientation are shown using the same format as in Figure 2 for TMS effects on spatial frequency selectivity. In Figure 3A, results are shown for a cell from which responses were obtained for seven spatial frequencies ($0.13\sim 1.2$ c/deg, evenly distributed on a logarithmic scale) for a total of 40 trials. A short TMS pulse train was applied just before the 16th trial (downward arrow), corresponding to time zero. Graphical results are shown in Figure 3B for spatial frequency tuning curves during pre- and post-TMS conditions, along with a recovery period. Data have been fit with the same equation as that for orientation tuning. However, since the spatial frequency axis (X-axis) is transformed to a

logarithmic scale, the fitted curve is not Gaussian shaped but has a longer tail on the left side. In the case of TMS induced suppression, as in this example, the area under the gray curve (post-TMS condition), is smaller than those under the other two curves. The fitting asymmetry causes TMS suppression to be more prominent at low compared to high spatial frequency ranges. In the recovery phase (dashed lines), the original tuning curve is nearly reproduced with slightly diminished response levels. Another example is shown in Figure 3C, D. Although the effect of TMS is similar to that of the previous example, the difference between low and high spatial frequencies is more accentuated. In this case, following TMS, high spatial frequencies yield slightly greater neural responses. The recovery curve is again similar to that prior to TMS, but the peak is slightly shifted to the right. A third example (Figure 3E, F) shows again the very unusual case of TMS induced facilitation in spatial frequency tuning. Note that the most extensive effects are exhibited at low spatial frequencies. Once again, the recovery data (dashed line) show a nearly identical, but slightly reduced, tuning curve as that prior to TMS.

TMS effects on contrast-response function: representative neurons

The third basic property of cortical tuning that we examined for TMS effects is contrast sensitivity. This is a fundamental tuning parameter and has been investigated in numerous studies of visual function [23–25]. Figure 4 contains three examples showing effects of TMS on contrast sensitivity. Display format is the same as the previous figures. In the first example (Figure 4A), neural responses are given for 10 different contrast values ranging from 5 to 100% evenly distributed on a logarithmic scale, and recorded in 40 trials. There is a steady gradual increase in response strength as contrast is increased. The sigmoid shaped response function, typical in contrast sensitivity measurements both behaviorally and neurophysiologically, is shown in Figure 4B. The curves here are fitted with a Naka-Rushton function (see Materials and Methods). The result of TMS application is a substantial suppression across the entire contrast range with an emphasis in the mid values (gray filled circles). Note that the suppression after TMS varies with contrast levels such that at low and high contrasts, effects are minimal and they are most extensive in the middle range. The subsequent recovery data (open circles with dashed line) is close to but still beneath the original control runs (black filled circles). Another example, Figure 4C & D, is similar to the previous cell. But TMS effects are more evenly distributed across a broad contrast range with minimal effects at the lowest levels. Note also that in this example, recovery data (dashed lines) are superimposed on original control responses with the exception of the highest contrast values tested. The third example, Figure 4E & F, shows a more linear contrast response function than in the previous cases. However, there is a striking difference in this case, because TMS has a facilitation effect rather than one of suppression and this is shown clearly throughout the range of contrasts tested except at 100%. For this example, the matrix in Figure 4E is missing a component from post-TMS time 12.5 to 22.5 minutes, because neural responses were not recorded during a recovery condition.

TMS effects on response selectivity based on spike activity: population data

Our next step is to determine if TMS effects on response selectivity, which we have shown here for representative cells, are general in our data population. To quantify TMS-induced

changes in orientation selectivity, we compare Gaussian fitting function parameters used for pre- and post-TMS conditions (Figure 5A). The main results derived from spike activities of 35 cells are as follows. First, a decrease of response magnitude is reflected in parameter K , which determines the height of the tuning curve (i.e., the maximum response). For most cells, parameter K in the pre-TMS condition is bigger than that for the post-TMS condition (Figure 5B) and the difference is statistically significant (Wilcoxon signed-rank test, $p < 0.001$), confirming that the our 4Hz rTMS is much more likely to cause suppression (filled triangles) than facilitation (open squares) of neural activity. TMS-induced suppression does not cause a horizontal shift (i.e., change of preferred orientation) of the tuning curve (Wilcoxon signed-rank test, $p = 0.41$, Figure 5C). However, TMS effects on orientation selectivity are not entirely explained by vertical scaling of the tuning curve of the pre-TMS condition. Strong suppression at non-preferred orientations often results in near-zero firing rates which are not different from spontaneous spike activity, so that the width of the orientation tuning curve becomes narrower (Wilcoxon signed-rank test, $p < 0.01$, Figure 5D). A smaller width of the tuning curve means that a cell responds to a more limited range of visual stimuli (i.e., sharp orientation tuning). Previous studies have suggested that intracortical inhibition contributes to neural response suppression and sharp orientation tuning [26–29]. We discuss below the role that intracortical inhibition may play in the observed TMS effects on orientation selectivity.

TMS-induced changes in spatial frequency tuning are similar to those observed for orientation tuning. First, 4Hz rTMS causes suppression of neural responses. Thus, parameter K , representing the maximum neural response, is significantly smaller in post-TMS condition than that in pre-TMS (Wilcoxon signed-rank test, $p < 0.001$, Figure 5F). Again, TMS-induced suppression and facilitation cases are expressed as filled triangles and open squares, respectively. Second, like preferred orientation, preferred spatial frequency associated with the strongest neural response is rarely changed by TMS (Wilcoxon signed-rank test, $p = 0.5$, data not shown). Furthermore, spatial frequency tuning width in a post-TMS condition tends to be smaller than that for pre-TMS. However, unlike orientation tuning, decreases of tuning width do not reach statistical significance (Wilcoxon signed-rank test, $p = 0.12$, data not shown).

An odd finding is that TMS-induced suppression is concentrated in the low frequency range. When spatial frequencies are higher than a cell's preferred value, neural response is minimally suppressed or even increased in some cases (Figure 3). To quantify this asymmetric effect of TMS on spatial frequency, we define the low and high spatial frequency cutoffs as lowest and highest spatial frequencies that yield neural activity stronger than half-maximum values of Gaussian-fitted spatial frequency tuning curves (Figure 5E). Our population data (32 cells) show that the low spatial frequency cutoffs in post-TMS conditions are significantly higher than those in pre-TMS (Wilcoxon signed-rank test, $p < 0.01$, Figure 5G). But the high spatial frequency cutoffs don't show systematic increases or decreases after TMS (Wilcoxon signed-rank test, $p = 0.88$, Figure 5H). These asymmetric changes in overall shape result in an emphasis on higher spatial frequencies.

As stimulus contrast varies from low to high, neural responses to the contrast varying stimulus are gradually increased until they are saturated at given contrast values. Therefore,

if a neural response is suppressed by TMS, the neuron requires a higher stimulus contrast to produce a response as strong as for the pre-TMS condition. We note that two different types of gain control can be involved in the suppression related change of the contrast-response function. If maximum neural responses (i.e., saturated neural responses) for pre- and post-TMS conditions are comparable, although they are produced at different contrast values, contrast-response functions in post-TMS conditions may be overlapped with rightward shifts of pre-TMS conditions. This case exemplifies contrast gain control [24,30]. On the other hand, if the maximum response in a post-TMS condition is lower than that for pre-TMS (even if response saturation for the two conditions occurs at similar contrast values), contrast tuning in post-TMS will be better explained by a vertical scaling rather than a horizontal shift of the pre-TMS condition. This case represents response gain control [31,32].

Among contrast tuning curve fitting parameters, R_{\max} and C_{50} are good indicators to judge which type of gain control is more relevant to TMS-induced suppression. R_{\max} and C_{50} represent the maximum (i.e., saturated) neural response and the stimulus contrast producing a half-maximum response, respectively. If response gain control is involved, R_{\max} is decreased but C_{50} is rarely affected. In the case of contrast gain control, on the other hand, C_{50} but not R_{\max} is changed.

Results from our population data (25 cells) confirms that TMS-induced suppression is likely to be mediated by contrast gain control. First, we don't find any meaningful difference between R_{\max} values of pre- and post-TMS conditions (Wilcoxon signed-rank test, $p=0.8$, Figure 5J). Data points above the diagonal line in Figure 5J are easy to be interpreted to represent TMS-induced facilitation. But this is true in only a minority of cases. If the neural response in a post-TMS condition is not fully saturated, even at the highest stimulus contrast, R_{\max} at that stage (even if it is suppressed (filled downward triangles)) can be larger than that for the pre-TMS condition. Second, C_{50} is significantly larger in the post-TMS compared to the pre-TMS condition (Wilcoxon signed-rank test, $p<0.01$, Figure 5L). However, the steepness (i.e., shape) is not systematically affected by TMS delivery (Wilcoxon signed-rank test, $p=0.51$, Figure 5K).

Discussion

In this study, we have investigated TMS effects on tuning properties of visual cortical neurons. To limit variables and obtain clear results, we have used a fixed delivery of TMS (4Hz, 4sec). We show that a short TMS pulse train generally induces prolonged but reversible suppression of neural activity. Our main finding is that response selectivity of individual neurons is significantly altered following delivery of TMS. Specifically, although the peaks of orientation tuning curves are rarely changed, there is strong suppression at non-preferred orientations which generally narrows the widths of the tuning curves. Suppression also occurs for spatial frequency tuning but effects are not symmetric regarding optimal spatial frequencies. Shapes of spatial frequency tuning curves tend to be altered primarily in low frequency ranges. Changes in contrast tuning curves are also found. They are explained by rightward horizontal shifts in response functions suggesting changes are mediated by contrast gain control. Finally, TMS-induced changes in spike responses are also observable in LFP signals, especially at high frequencies (70~100 Hz, see Supplementary Materials).

TMS effects: Suppression vs. Facilitation

Although the dominant effect of our 4Hz rTMS is suppression, facilitative effects are also occasionally observed (12 out of 92 cells). TMS-induced facilitation shows a similar time course of neural activity change as with suppression but in an opposite direction. In general, TMS modulates cortical activity in a frequency-dependent manner [33–36]. Findings include reduced cortical activity following low frequency (1Hz) and increased levels after high frequency stimulation (>10Hz). The stimulation frequency we used is at a mid-level (4Hz), which may be near the border of overlap between suppression and facilitation. In addition, magnetic coil position may affect findings of suppression and facilitation. In the visual cortex, TMS-induced suppression may require stimulation of stronger intensity than that for facilitation [37–40], although we need to keep in mind that effects of stimulus intensity may be different for single pulse TMS and rTMS conditions. Since the intensity of the magnetic field induced by TMS decreases exponentially with distance from the coil [41], when a coil is positioned away from the skull, a high stimulus intensity may cause facilitation instead of suppression. And neurons in deeper cortical layers may be more facilitated than those in superficial regions.

Although we do not have histological identification of specific cortical lamina, we can use recording depths to infer layers as done in previous work [42]. Studies have shown that the major recipient of input from LGN is layer 4 which consists mainly of simple type cells [43,44]. Complex cells reside mainly in upper and deeper layers [45–47]. We have used our cortical depth information along with standard physiological observations to infer populations of simple and complex cells. Our results show that effects of TMS are not significantly different for simple and complex cells.

In a simulation study, magnetic stimulation (MS) induces the largest depolarization at the soma. Increasing the diameter of the soma reduces the magnetic threshold for action potential generation [48]. In addition to the diameter of the soma, number (or size) of axons may be an important feature which determines different TMS effects. Extracellular electrical stimulation in cortical gray matter directly activates axons but not cell bodies [49]. And the soma is much more difficult to excite than the axon [50,51]. These results suggest differences of activation of cortical neurons that depend on TMS parameters. However, a detailed relationship of these factors to TMS-induced suppression or facilitation is not currently available.

In our study, facilitation cases are relatively rare, so there is not sufficient data to draw a meaningful relationship with cell types. Other work could be undertaken in which different stimulation frequencies and intensities can be used independently to determine details of occurrence of TMS-induced facilitation.

Long lasting effects of repetitive TMS

TMS can be applied with single stimulation (single-pulse TMS), or as pairs of stimuli with one or more coils (paired-pulse TMS), or as multiple stimuli in trains (repetitive TMS or rTMS) [8]. Depending on parameters (e.g., intensity, duration, inter-stimulus interval, etc.), cortical excitability can be increased or decreased [33,34,36,52,53]. Compared with other

protocols, a main characteristic of rTMS is that it can induce long-term changes of cortical excitability [8]. This has led to use of rTMS as a noninvasive treatment in psychiatry. rTMS has been reported to be effective for depression, bipolar disorder, schizophrenia, aphasia, and chronic pain [7,8]. However, clinical applications rely on empirical findings that are not based on underlying neural mechanisms.

One can differentiate rTMS into two different protocols, ‘conventional’ and ‘patterned’ rTMS [8]. Conventional rTMS refers to the application of regularly repeated single TMS pulses. In a patterned protocol, repetitive application of short rTMS bursts with high inner frequencies is interleaved with short pauses of no stimulation. The latter method is relatively new and may have some advantages over the conventional type in that it can induce similar changes in cortical excitability with shorter stimulus trains and lower intensities [54]. However, this method also has a higher risk of causing seizures than other rTMS protocols [55], so it must be applied with caution.

Using the combined approach of electrophysiology and rTMS, we previously have shown that short TMS pulse trains (conventional rTMS; 4Hz, 4sec) can cause neural response suppression for sustained period. As a next step, we report here that basic response selectivities of neurons in visual cortex are altered during this time. Since response selectivity involves feedforward and intracortical connections [26–29,56], TMS must affect these pathways as considered below.

Neural mechanisms involved in orientation tuning

Feedforward convergence from multiple LGN cells to a V1 neuron determines preferred orientation. Thalamocortical synapses are thought to be purely excitatory [57,58]. Therefore, for a given spike threshold, orientation tuning for high contrasts should be broader than that for low. A feedforward-only mechanism cannot produce sharp orientation tuning. And it cannot explain a contrast-invariant characteristic [59,60]. Previous studies of orientation tuning at different response latencies show that tuning width is decreased during the response [27,61]. This is due to inhibitory inputs from neighboring cortical neurons that are delayed compared to feedforward inputs from LGN.

TMS effects on orientation selectivity (diminished neural responses & narrowed tuning width) are similar to changes expected when intracortical inhibitions are activated. In addition, TMS effects are somewhat analogous to those of visual adaptation in that both effects are reversible. However, unlike adaptation-induced plasticity of orientation tuning which follows exposure to a given value and results in a peak orientation shift [62,63], TMS application does not target a single orientation, so it does not alter preferred angles.

We used 10 different orientation values covering a 90 deg range to quantify orientation selectivity of an individual neuron. This method excludes a vector summation analysis which could also provide a measurement of orientation selectivity. We note that in our analysis, a lack of shift of preferred orientation is a solid finding and not due to an artifact. In our data population, mean value of orientation tuning width (parameter σ) is about 15 deg (see Figure 5). This means that for most cells, visual responses are reduced to zero at both ends of tested orientation range (see Figure 2). The vector summation method would not

provide meaningful additional information for preferred direction of motion. We should also note that we did not test orientation selectivity in non-preferred directions since responses for this variable are generally very low.

Stronger suppression in low spatial frequency range

The main TMS effect for spatial frequency tuning is an asymmetric change in overall shape. Low but not high spatial frequency cutoff is significantly increased. These results suggest distinct neural circuits responsible for low and high spatial frequency processing.

A large proportion of LGN neurons show low-pass spatial frequency tuning, whereas most neurons in visual cortex have band-pass characteristics [56,64,65]. The transition from low- to band-pass spatial frequency tuning, like that from broad to sharp orientation tuning, may require intracortical inhibitory interneurons [66]. Visual cortical neurons show temporal dynamics in spatial frequency tuning. The preferred spatial frequency shifts from low to high values [67–69]. Our finding of stronger TMS-induced suppression in the low spatial frequency range may be related to these previous results. The short TMS pulse train applied to visual cortex may disrupt the balance between feedforward excitatory inputs from LGN and inputs from intracortical connections. Increased contribution of intracortical connections may result in diminished neural activity in the low spatial frequency range.

Contrast gain control

Cortical cells maintain sensitivity over a wide range of contrast by centering response range to specific local levels [24,30]. This contrast gain control process is reflected by a horizontal shift of the contrast-response function.

TMS effects on the contrast-response function (increased C_{50} and unaffected R_{max}) are better explained by a rightward horizontal shift rather than a vertical scaling of the original function. This suggests that TMS-induced suppression may be mediated by a contrast gain control mechanism.

Contrast gain control is thought to be generated at an input stage [70,71]. Therefore, post-TMS neural response may be similar to that for a low contrast stimulus. However, this is at odds with previous findings and our current results. First, cortical orientation selectivity has a contrast-invariant property [59,60], but TMS-induced suppression narrows the width of orientation tuning curves.

Second, spatial frequency tuning for low contrast accentuates low spatial frequencies [72]. But TMS-induced suppression is stronger at low frequencies and neural responses to high frequencies are minimally altered. Contrast adaptation typically results in horizontal shifts of the contrast-response function [24,30,73–75]. Therefore, short TMS pulse trains cause an effect similar to what is expected if a population of cortical cells, which covers all orientations and a broad range of spatial & temporal frequencies, is adapted to a high contrast stimulus.

Limitations of current study

We have used a single parameter set for the current work to reduce possible variables. We should note that effects may be different for various cell types. If various cell types can be selectively affected by TMS with different parameters (intensity, frequency, duration, and so on), this would provide useful information.

It is also worth examining TMS effects on temporal dynamics of functional tuning. This analysis requires a reverse correlation method, which is more time consuming than what we have used in the current study. However, even under the assumption that TMS may induce larger contributions of intra-cortical processing, it does not necessarily follow that TMS effects on response selectivity are only observable at delayed response latency. Without TMS application, intra-cortical inhibition is forced to be later than feedforward input. However, if TMS causes a different neuronal state (e.g., elevated intra-cortical inhibition even before visual stimulation), TMS effects on response selectivity may occur from the earliest response latency.

Exact recovery times can be studied by detailed examination of relatively late trials (31st~40th trials in our protocol) following the post-TMS condition. We showed here that TMS effects are not permanent and that their influence on response selectivity gets weaker at delayed phases.

It is also desirable to determine if our results obtained in anesthetized animals can be translated into human TMS studies. Our stimulation parameters are somewhat different from those generally used for human rTMS. Most human studies tend to involve weaker stimulation intensities, but longer durations than what we have used here [8]. Effects of TMS in humans have been reported to last up to several hours [76–78]. TMS – fMRI combined studies may provide correlations between TMS-induced behavioral changes and hemodynamic alterations in functionally related brain regions.

Conclusions

Short rTMS pulses (4Hz, 4sec) applied over the cat's visual cortex cause long-lasting reversible changes in neural activity. Neural responses to visual stimuli generally are clearly suppressed after TMS application and they gradually recover to levels close to pre-TMS conditions during 10~15 minute periods. Facilitative effects are observed in a small number of cases (12 out of 92). The TMS-induced changes in neural responses are reflected at both input (LFPs) and output (spike activity) stages of cortical processing. These effects are accompanied by substantial changes in response selectivity including: sharper orientation tuning, selective suppression at low spatial frequencies, and response saturation at higher contrast values. These findings suggest that TMS interrupts the existing balance between sub-cortical and intra-cortical inputs for relatively extended time periods.

Supplementary Material

Refer to Web version on PubMed Central for supplementary material.

Acknowledgments

We thank Prof. Richard Ivry for the loan of TMS equipment. The authors declare no competing financial interests. This research is supported by NIH grant EY01175.

References

- [1]. Goddard G, McIntyre D, Leech C. A permanent change in brain function resulting from daily electrical stimulation. *Exp Neurol*. 1969; 25:295–330. doi:10.1016/0014-4886(69)90128-9. [PubMed: 4981856]
- [2]. Racine R. Modification of seizure activity by electrical stimulation: II. Motor seizure. *Electroencephalogr Clin Neurophysiol*. 1972; 32:281–94. doi:10.1016/0013-4694(72)90177-0. [PubMed: 4110397]
- [3]. Merton P, Morton H. Stimulation of the cerebral cortex in the intact human subject. *Nature*. 1980; 285:227. doi:10.1038/285227a0. [PubMed: 7374773]
- [4]. Barker A, Jalinous R, Freeston I. Non-invasive magnetic stimulation of human motor cortex. *Lancet*. 1985; 1:1106–7. doi:10.1016/S0140-6736(85)92413-4. [PubMed: 2860322]
- [5]. Pascual-Leone A, Nguyet D, Cohen LG, Brasil-Neto JP, Cammarota A, Hallett M. Modulation of muscle responses evoked by transcranial magnetic stimulation during the acquisition of new fine motor skills. *J Neurophysiol*. 1995; 74:1037–45. [PubMed: 7500130]
- [6]. Hallett M. Transcranial magnetic stimulation and the human brain. *Nature*. 2000; 406:147–50. doi:10.1038/35018000. [PubMed: 10910346]
- [7]. Wassermann E, Lisanby S. Therapeutic application of repetitive transcranial magnetic stimulation: a review. *Clin Neurophysiol*. 2001; 112:1367–77. doi:10.1016/S1388-2457(01)00585-5. [PubMed: 11459676]
- [8]. Rossi S, Hallett M, Rossini PM, Pascual-Leone A. Safety, ethical considerations, and application guidelines for the use of transcranial magnetic stimulation in clinical practice and research. *Clin Neurophysiol*. 2009; 120:2008–39. doi:10.1016/j.clinph.2009.08.016. [PubMed: 19833552]
- [9]. Pascual-Leone A, Valls-Solé J, Wassermann EM, Hallett M. Responses to rapid-rate transcranial magnetic stimulation of the human motor cortex. *Brain*. 1994; 117(Pt 4):847–58. [PubMed: 7922470]
- [10]. Chen R, Classen J, Gerloff C, Celnik P, Wassermann EM, Hallett M, et al. Depression of motor cortex excitability by low-frequency transcranial magnetic stimulation. *Neurology*. 1997; 48:1398–403. doi:10.1212/WNL.48.5.1398. [PubMed: 9153480]
- [11]. Nakamura H, Kitagawa H, Kawaguchi Y, Tsuji H. Intracortical facilitation and inhibition after transcranial magnetic stimulation in conscious humans. 1997; 498(Pt 3.)
- [12]. Peinemann A, Reimer B, L??er C, Quartarone A, M??nchau A, Conrad B, et al. Long-lasting increase in corticospinal excitability after 1800 pulses of subthreshold 5 Hz repetitive TMS to the primary motor cortex. *Clin Neurophysiol*. 2004; 115:1519–26. doi:10.1016/j.clinph.2004.02.005. [PubMed: 15203053]
- [13]. Valls-Sole J, Pascual-Leone A, Brasil-Neto JP, Cammarota A, McShane L, Hallett M. Abnormal facilitation of the response to transcranial magnetic stimulation in patients with Parkinson's disease. *Neurology*. 1994; 44:735–735. doi:10.1212/WNL.44.4.735. [PubMed: 8164834]
- [14]. Maeda F, Keenan JP, Tormos JM, Topka H, Pascual-Leone A. Interindividual variability of the modulatory effects of repetitive transcranial magnetic stimulation on cortical excitability. *Exp Brain Res*. 2000; 133:425–30. doi:10.1007/s002210000432. [PubMed: 10985677]
- [15]. Siebner HR, Lang N, Rizzo V, Nitsche MA, Paulus W, Lemon RN, et al. Preconditioning of low-frequency repetitive transcranial magnetic stimulation with transcranial direct current stimulation: evidence for homeostatic plasticity in the human motor cortex. *J Neurosci*. 2004; 24:3379–85. doi:10.1523/JNEUROSCI.5316-03.2004. [PubMed: 15056717]
- [16]. Silvanto J, Muggleton NG, Cowey A, Walsh V. Neural adaptation reveals state-dependent effects of transcranial magnetic stimulation. *Eur J Neurosci*. 2007; 25:1874–81. doi:10.1111/j.1460-9568.2007.05440.x. [PubMed: 17408427]

- [17]. Pasley B, Allen E, Freeman R. State-dependent variability of neuronal responses to transcranial magnetic stimulation of the visual cortex. *Neuron*. 2009; 62:291–303. doi:10.1016/j.neuron.2009.03.012. [PubMed: 19409273]
- [18]. Allen EA, Pasley BN, Duong T, Freeman RD. Transcranial magnetic stimulation elicits coupled neural and hemodynamic consequences. *Science*. 2007; 317:1918–21. doi:10.1126/science.1146426. [PubMed: 17901333]
- [19]. Hotson J, Braun D, Herzberg W, Boman D. Transcranial magnetic stimulation of extrastriate cortex degrades human motion direction discrimination. *Vision Res*. 1994; 34:2115–23. [PubMed: 7941409]
- [20]. Silvanto J, Muggleton N, Walsh V. State-dependency in brain stimulation studies of perception and cognition. *Trends Cogn Sci*. 2008; 12:447–54. doi:10.1016/j.tics.2008.09.004. [PubMed: 18951833]
- [21]. Cattaneo Z, Rota F, Walsh V, Vecchi T, Silvanto J. TMS-adaptation reveals abstract letter selectivity in the left posterior parietal cortex. *Cereb Cortex*. 2009; 19:2321–5. doi:10.1093/cercor/bhn249. [PubMed: 19150919]
- [22]. Salinas FS, Lancaster JL, Fox PT. Detailed 3D models of the induced electric field of transcranial magnetic stimulation coils. *Phys Med Biol*. 2007; 52:2879–92. doi:10.1088/0031-9155/52/10/016. [PubMed: 17473357]
- [23]. Albrecht D, Hamilton D. Striate cortex of monkey and cat: contrast response function. *J Neurophysiol*. 1982; 48:217–37. [PubMed: 7119846]
- [24]. Ohzawa I, Sclar G, Freeman R. Contrast gain control in the cat visual cortex. *Nature*. 1982; 298:266–8. doi:10.1038/298266a0. [PubMed: 7088176]
- [25]. Sceniak MP, Ringach DL, Hawken MJ, Shapley R. Contrast's effect on spatial summation by macaque V1 neurons. *Nat Neurosci*. 1999; 2:733–9. doi:10.1038/11197. [PubMed: 10412063]
- [26]. Sillito A. The contribution of inhibitory mechanisms to the receptive field properties of neurones in the striate cortex of the cat. *J Physiol*. 1975; 250:305–29. [PubMed: 1177144]
- [27]. Chen G, Dan Y, Li C. Stimulation of non-classical receptive field enhances orientation selectivity in the cat. *J Physiol*. 2005; 564:233–43. doi:10.1113/jphysiol.2004.080051. [PubMed: 15677690]
- [28]. Shapley R, Hawken M, Xing D. The dynamics of visual responses in the primary visual cortex. *Prog Brain Res*. 2007; 165:21–32. doi:10.1016/S0079-6123(06)65003-6. [PubMed: 17925238]
- [29]. Okamoto M, Naito T, Sadakane O, Osaki H, Sato H. Surround suppression sharpens orientation tuning in the cat primary visual cortex. *Eur J Neurosci*. 2009; 29:1035–46. doi:10.1111/j.1460-9568.2009.06645.x. [PubMed: 19291228]
- [30]. Ohzawa I, Sclar G, Freeman R. Contrast gain control in the cat's visual system. *J Neurophysiol*. 1985; 54:651–67. [PubMed: 4045542]
- [31]. Sengpiel F, Baddeley RJ, Freeman TCB, Harrad R, Blakemore C. Different mechanisms underlie three inhibitory phenomena in cat area 17. *Vision Res*. 1998; 38:2067–80. doi:10.1016/S0042-6989(97)00413-6. [PubMed: 9797967]
- [32]. Reynolds J, Pasternak T, Desimone R. Attention increases sensitivity of V4 neurons. *Neuron*. 2000; 26:703–14. doi:10.1016/S0896-6273(00)81206-4. [PubMed: 10896165]
- [33]. Aydin-Abidin S, Moliadze V, Eysel UT, Funke K. Effects of repetitive TMS on visually evoked potentials and EEG in the anaesthetized cat: dependence on stimulus frequency and train duration. *J Physiol*. 2006; 574:443–55. doi:10.1113/jphysiol.2006.108464. [PubMed: 16690713]
- [34]. Hallett M. Transcranial magnetic stimulation: a primer. *Neuron*. 2007; 55:187–99. doi:10.1016/j.neuron.2007.06.026. [PubMed: 17640522]
- [35]. Valero-Cabre A, Payne BR, Pascual-Leone A. Opposite impact on (14)C-2-deoxyglucose brain metabolism following patterns of high and low frequency repetitive transcranial magnetic stimulation in the posterior parietal cortex. *Exp Brain Res*. 2007; 176:603–15. [PubMed: 16972076]
- [36]. Eldaief MC, Halko MA, Buckner RL, Pascual-Leone A. Transcranial magnetic stimulation modulates the brain's intrinsic activity in a frequency-dependent manner. *Proc Natl Acad Sci*. 2011; 108:21229–34. doi:10.1073/pnas.1113103109. [PubMed: 22160708]

- [37]. Moliadze V, Zhao Y, Eysel U, Funke K. Effect of transcranial magnetic stimulation on single-unit activity in the cat primary visual cortex. *J Physiol.* 2003; 553:665–79. doi:10.1113/jphysiol.2003.050153. [PubMed: 12963791]
- [38]. Kammer T, Puls K, Erb M, Grodd W. Transcranial magnetic stimulation in the visual system. II. Characterization of induced phosphenes and scotomas. *Exp Brain Res.* 2005; 160:129–40. doi:10.1007/s00221-004-1992-0. [PubMed: 15368087]
- [39]. Garry MI, Thomson RHS. The effect of test TMS intensity on short-interval intracortical inhibition in different excitability states. *Exp Brain Res.* 2009; 193:267–74. doi:10.1007/s00221-008-1620-5. [PubMed: 18974984]
- [40]. Schwarzkopf DS, Silvanto J, Rees G. Stochastic resonance effects reveal the neural mechanisms of transcranial magnetic stimulation. *J Neurosci.* 2011; 31:3143–7. doi:10.1523/JNEUROSCI.4863-10.2011. [PubMed: 21368025]
- [41]. George MS, Lisanby SH, Sackeim HA. Transcranial magnetic stimulation: applications in neuropsychiatry. *Arch Gen Psychiatry.* 1999; 56:300–11. doi:10.1001/archpsyc.56.4.300. [PubMed: 10197824]
- [42]. Ringach DL, Shapley RM, Hawken MJ. Orientation selectivity in macaque V1: diversity and laminar dependence. *J Neurosci.* 2002; 22:5639–51. doi:20026567. [PubMed: 12097515]
- [43]. McGuire BA, Hornung JP, Gilbert CD, Wiesel TN. Patterns of synaptic input to layer 4 of cat striate cortex. *J Neurosci.* 1984; 4:3021–33. [PubMed: 6502220]
- [44]. LeVay S, Gilbert CD. Laminar patterns of geniculocortical projection in the cat. *Brain Res.* 1976; 113:1–19. doi:10.1016/0006-8993(76)90002-0. [PubMed: 953720]
- [45]. Alonso JM, Martinez LM. Functional connectivity between simple cells and complex cells in cat striate cortex. *Nat Neurosci.* 1998; 1:395–403. doi:10.1038/1609. [PubMed: 10196530]
- [46]. Martinez LM, Wang Q, Reid RC, Pillai C, Alonso J-M, Sommer FT, et al. Receptive field structure varies with layer in the primary visual cortex. *Nat Neurosci.* 2005; 8:372–9. doi:10.1038/nn1404. [PubMed: 15711543]
- [47]. Gilbert CD. Laminar differences in receptive field properties of cells in cat primary visual cortex. *J Physiol.* 1977; 268:391–421. [PubMed: 874916]
- [48]. Pashut T, Wolfus S, Friedman A, Lavidor M, Bar-Gad I, Yeshurun Y, et al. Mechanisms of magnetic stimulation of central nervous system neurons. *PLoS Comput Biol.* 2011; 7:e1002022. doi:10.1371/journal.pcbi.1002022. [PubMed: 21455288]
- [49]. Nowak LG, Bullier J. Axons, but not cell bodies, are activated by electrical stimulation in cortical gray matter. I. Evidence from chronaxie measurements. *Exp Brain Res.* 1998; 118:477–88. doi:10.1007/s002210050304. [PubMed: 9504843]
- [50]. Rattay F. The basic mechanism for the electrical stimulation of the nervous system. *Neuroscience.* 1999; 89:335–46. doi:10.1016/S0306-4522(98)00330-3. [PubMed: 10077317]
- [51]. McIntyre CC, Grill WM. Excitation of central nervous system neurons by nonuniform electric fields. *Biophys J.* 1999; 76:878–88. doi:10.1016/S0006-3495(99)77251-6. [PubMed: 9929489]
- [52]. Fierro B, Brighina F, Vitello G, Piazza A, Scalia S, Giglia G, et al. Modulatory effects of low- and high-frequency repetitive transcranial magnetic stimulation on visual cortex of healthy subjects undergoing light deprivation. *J Physiol.* 2005; 565:659–65. doi:10.1113/jphysiol.2004.080184. [PubMed: 15760946]
- [53]. Funke K, Benali A. Modulation of cortical inhibition by rTMS—findings obtained from animal models. *J Physiol.* 2011; 589:4423–35. doi:10.1113/jphysiol.2011.206573. [PubMed: 21768267]
- [54]. Platz T, Rothwell JC. Brain stimulation and brain repair—rTMS: from animal experiment to clinical trials—what do we know? *Restor Neurol Neurosci.* 2010; 28:387–98. doi:10.3233/RNN-2010-0570. [PubMed: 20714064]
- [55]. Oberman L, Edwards D, Eldaief M, Pascual-Leone A. Safety of theta burst transcranial magnetic stimulation: a systematic review of the literature. *J Clin Neurophysiol.* 2011; 28:67–74. doi:10.1097/WNP.0b013e318205135f. [PubMed: 21221011]
- [56]. Bredfeldt C, Ringach D. Dynamics of spatial frequency tuning in macaque V1. *J Neurosci.* 2002; 22:1976–84. [PubMed: 11880528]
- [57]. Freund TF, Martin KA, Soltesz I, Somogyi P, Whitteridge D. Arborisation pattern and postsynaptic targets of physiologically identified thalamocortical afferents in striate cortex of the

- macaque monkey. *J Comp Neurol.* 1989; 289:315–36. doi:10.1002/cne.902890211. [PubMed: 2808770]
- [58]. Kharazia V, Weinberg R. Glutamate in thalamic fibers terminating in layer IV of primary sensory cortex. *J Neurosci.* 1994; 14:6021–32. [PubMed: 7931559]
- [59]. Sclar G, Freeman R. Orientation selectivity in the cat's striate cortex is invariant with stimulus contrast. *Exp Brain Res.* 1982; 46:457–61. doi:10.1007/BF00238641. [PubMed: 7095050]
- [60]. Troyer TW, Krukowski AE, Priebe NJ, Miller KD. Contrast-invariant orientation tuning in cat visual cortex: thalamocortical input tuning and correlation-based intracortical connectivity. *J Neurosci.* 1998; 18:5908–27. [PubMed: 9671678]
- [61]. Ringach D, Hawken M, Shapley R. Dynamics of orientation tuning in macaque primary visual cortex. *Nature.* 1997; 387:281–4. doi:10.1038/387281a0. [PubMed: 9153392]
- [62]. Dragoi V, Sharma J, Sur M. Adaptation-induced plasticity of orientation tuning in adult visual cortex. *Neuron.* 2000; 28:287–98. doi:10.1016/S0896-6273(00)00103-3. [PubMed: 11087001]
- [63]. Ghisovan N, Nemri A, Shumikhina S, Molotchnikoff S. Long adaptation reveals mostly attractive shifts of orientation tuning in cat primary visual cortex. *Neuroscience.* 2009; 164:1274–83. doi: 10.1016/j.neuroscience.2009.09.003. [PubMed: 19747528]
- [64]. Maffei L, Fiorentini A. The visual cortex as a spatial frequency analyser. *Vision Res.* 1973; 13:1255–67. doi:10.1016/0042-6989(73)90201-0. [PubMed: 4722797]
- [65]. De Valois KK, Tootell RB. Spatial-frequency-specific inhibition in cat striate cortex cells. *J Physiol.* 1983; 336:359–76. [PubMed: 6875912]
- [66]. Bauman LA, Bonds AB. Inhibitory refinement of spatial frequency selectivity in single cells of the cat striate cortex. *Vision Res.* 1991; 31:933–44. doi:10.1016/0042-6989(91)90201-F. [PubMed: 1858324]
- [67]. Mazer JA, Vinje WE, McDermott J, Schiller PH, Gallant JL. Spatial frequency and orientation tuning dynamics in area V1. *Proc Natl Acad Sci U S A.* 2002; 99:1645–50. doi:10.1073/pnas.022638499. [PubMed: 11818532]
- [68]. Frazor RA, Albrecht DG, Geisler WS, Crane AM. Visual cortex neurons of monkeys and cats: temporal dynamics of the spatial frequency response function. *J Neurophysiol.* 2004; 91:2607–27. doi:10.1152/jn.00858.2003. [PubMed: 14960559]
- [69]. Allen EA, Freeman RD. Dynamic spatial processing originates in early visual pathways. *J Neurosci.* 2006; 26:11763–74. doi:10.1523/JNEUROSCI.3297-06.2006. [PubMed: 17093097]
- [70]. Carandini M. Visual cortex: Fatigue and adaptation. *Curr Biol.* 2000; 10 doi:10.1016/S0960-9822(00)00637-0.
- [71]. Katzner S, Busse L, Carandini M. GABAA inhibition controls response gain in visual cortex. *J Neurosci.* 2011; 31:5931–41. doi:10.1523/JNEUROSCI.5753-10.2011. [PubMed: 21508218]
- [72]. Sceniak MP, Hawken MJ, Shapley R. Contrast-dependent changes in spatial frequency tuning of macaque V1 neurons: effects of a changing receptive field size. *J Neurophysiol.* 2002; 88:1363–73. doi:10.1152/jn.00967.2001. [PubMed: 12205157]
- [73]. Bonds A. Temporal dynamics of contrast gain in single cells of the cat striate cortex. *Vis Neurosci.* 1991; 6:239–55. [PubMed: 2054326]
- [74]. Carandini M, Ferster D. A tonic hyperpolarization underlying contrast adaptation in cat visual cortex. *Science (80-).* 1997; 276:949–52. doi:10.1126/science.276.5314.949.
- [75]. Gardner JL, Sun P, Waggoner RA, Ueno K, Tanaka K, Cheng K. Contrast adaptation and representation in human early visual cortex. *Neuron.* 2005; 47:607–20. doi:10.1016/j.neuron.2005.07.016. [PubMed: 16102542]
- [76]. Pascual-Leone A, Tormos JM, Keenan J, Tarazona F, Canete C, Catala MD. Study and modulation of human cortical excitability with transcranial magnetic stimulation. *J Clin Neurophysiol.* 1998; 15:333–43. [PubMed: 9736467]
- [77]. Huang Y-Z, Edwards MJ, Rounis E, Bhatia KP, Rothwell JC. Theta burst stimulation of the human motor cortex. 2005; 45 doi:10.1016/j.neuron.2004.12.033.
- [78]. Ziemann U, Paulus W, Nitsche MA, Pascual-Leone A, Byblow WD, Berardelli A, et al. Consensus: Motor cortex plasticity protocols. *Brain Stimul.* 2008; 1:164–82. doi:10.1016/j.brs.2008.06.006. [PubMed: 20633383]

Highlights

- rTMS (4Hz, 4sec) causes long-lasting changes in functional tunings of visual neurons
- TMS-induced suppression narrows the width of orientation tuning curves
- Response suppression is greater in low spatial frequency range
- Contrast-response functions saturate at higher contrast values

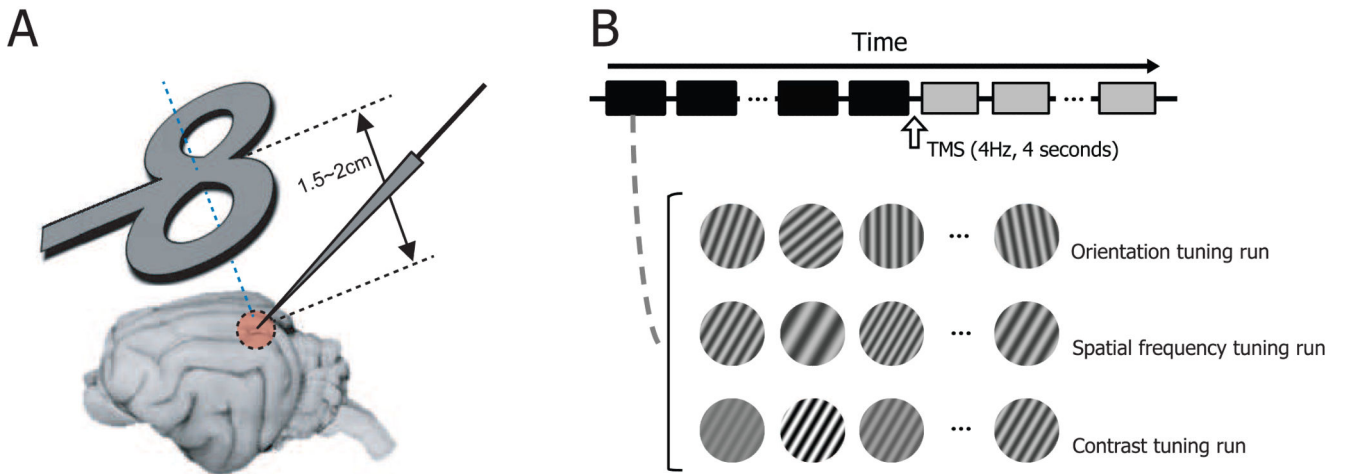


Figure 1.

Experimental paradigm. **A.** Figure-8 coil is positioned obliquely near the transverse plane superior to the visual cortex (1.5~2cm apart from the cortical surface). Its midpoint is aligned to the left visual cortex craniotomy (Horsley-Clarke coordinates P4 L2). Tungsten electrode penetration is made at an angle of A45, M0. **B.** We examine how rTMS alters selectivity of cells in the visual cortex. To do this, we measure orientation, spatial frequency, and contrast tuning properties of cells and compare the properties between pre- and post-TMS conditions. For orientation tuning run, 7~10 differently oriented circular grating patches (stimulus duration: 2 seconds, inter-stimulus interval: 2 seconds) are presented in a cell's classical receptive field in each trial (depicted as squares below the time arrow). 4Hz TMS pulse train is delivered for 4 seconds in the inter-trial interval (10 seconds) between 15th and 16th trials. Black and gray colors are used to represent pre- and post-TMS conditions, respectively.

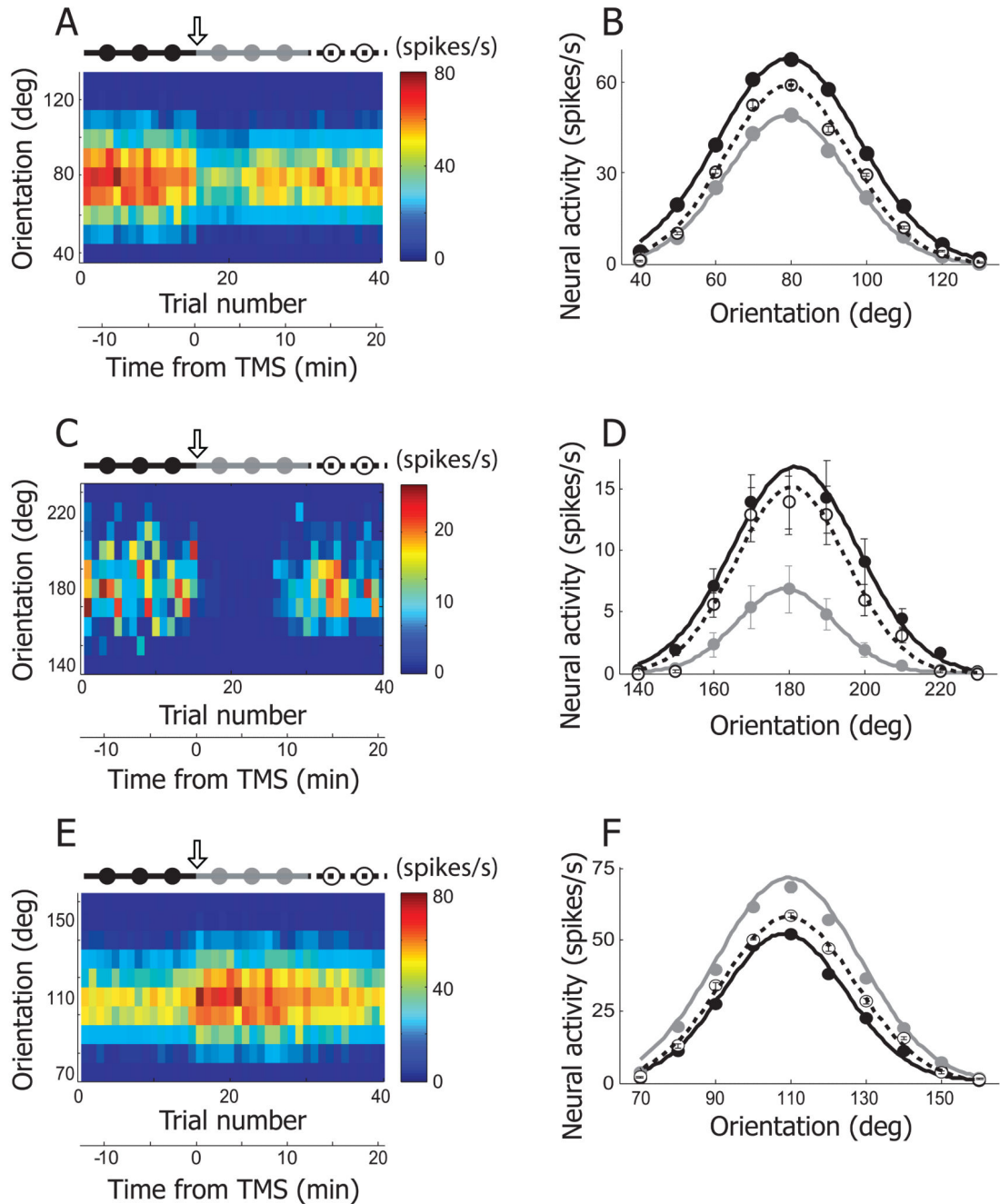


Figure 2.

Three examples showing TMS effects on orientation selectivity. **A.** Neural response of an example cell is depicted as a form of matrix. X- and Y-axis indicate trial number and orientation, respectively. In each trial (column), 10 different orientations (40~130°, 10° step) were tested. Response magnitude is coded with colors on a blue-red scale. 4Hz rTMS (downward arrow) was delivered for 4 seconds just before the 16th trial. The total 40 trials are divided into three groups based on elapsed time from TMS delivery: pre-TMS (1~15th trials, black filled circles and line), post-TMS (16~30th trials, gray filled circles and line),

and recovery (31~40th trials, open circles and dotted line) conditions. Trial number was translated into time from TMS delivery. Neural response was abruptly changed as soon as TMS was applied. The TMS effect was reversible and it lasted for approximately 10 minutes. **B.** Three orientation tuning curves were created from the cell depicted in (A). Black, gray, and open circles are mean neural responses for 10 different orientations computed in pre-TMS, post-TMS, and recovery conditions, respectively. Error bar indicates standard error of mean. Error bars are smaller than circles when not visible. In these three conditions, the preferred orientation is not changed but response magnitude is clearly diminished in post-TMS condition compared with the other two conditions. More detailed analysis of TMS-effects on orientation selectivity will be dealt in Figure 5A~D. **C, D.** Another example cell showing TMS effects on orientation selectivity. The same conventions are used as in (A), (B). The black circle at 180° is hidden by the open one. **E, F.** Our rTMS (4Hz, 4sec) mainly caused prolonged suppression of neural responses in cat's visual cortex (80 out of 92 units). But, in small cases, TMS-induced facilitation was also observable. One example is introduced here.

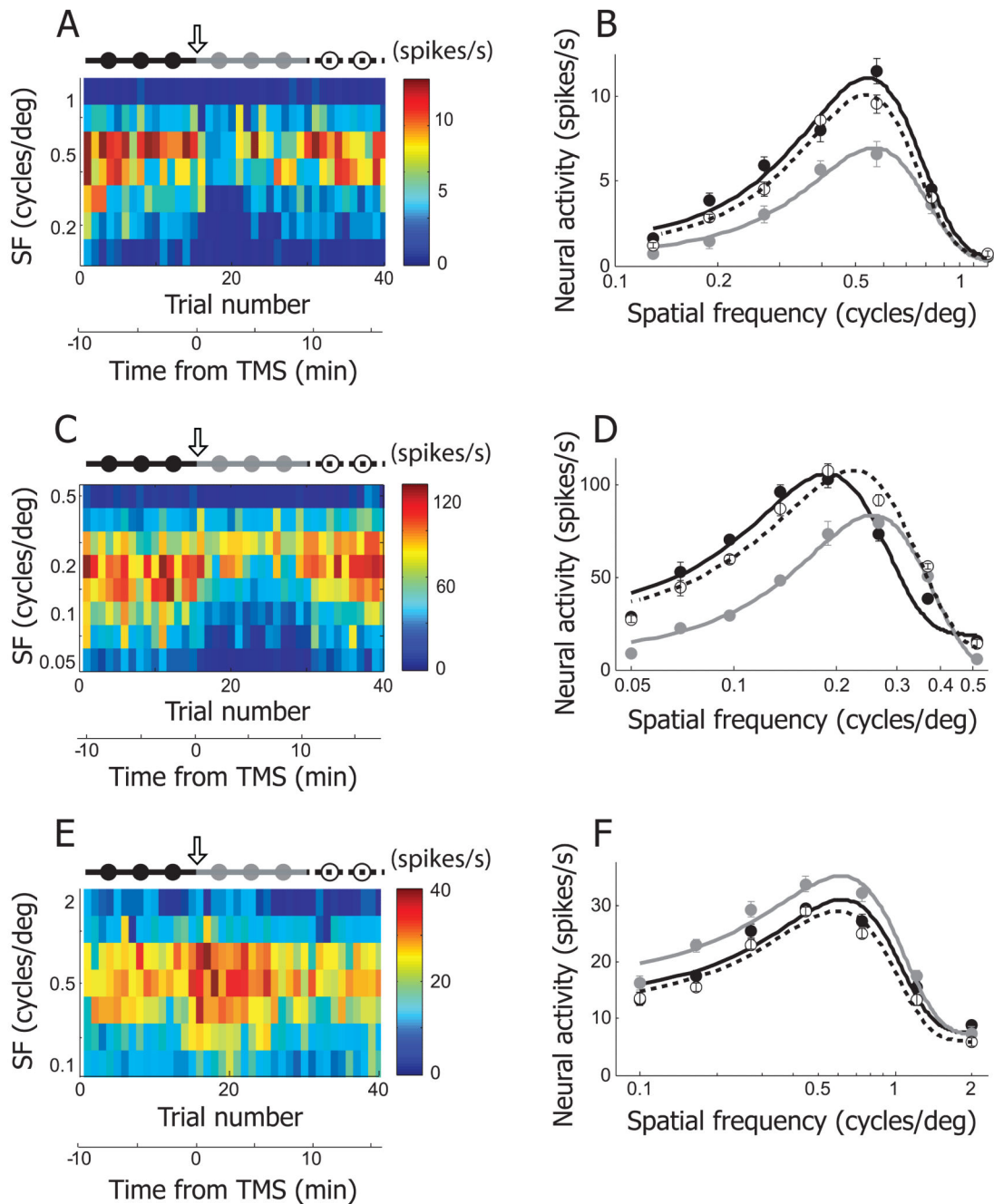


Figure 3.

Three examples showing TMS effects on spatial frequency selectivity. **A.** In this example cell, neural responses for 7 different spatial frequencies (0.13~1.2 c/deg, evenly distributed in logarithmic scale) were recorded in 40 trials. The plotting conventions are the same as in Figure 2A. 4Hz rTMS (downward arrow) was applied just before the 16th trial. The total 40 trials are divided into three groups to create tuning functions in pre-TMS (1~15th trials, black filled circles and line), post-TMS (16~30th trials, gray filled circles and line), and recovery (31~40th trials, open circles and dotted line) conditions. **B.** Spatial frequency

tuning curves of pre-TMS, post-TMS and recovery conditions were created from the cell depicted in (A). Equation used for curve fitting is the same as the one used for orientation tuning. But spatial frequency tuning curve is not Gaussian shaped, because x-axis is transformed to logarithmic scale. The area under the gray curve (post-TMS condition) is smaller than those under the other two curves. Note that TMS-induced suppression is more apparent in low spatial frequency range than high spatial frequency range. More detailed analysis of TMS-effects on spatial frequency selectivity will be dealt in Figure 5E~H. **C, D.** Another example cell showing TMS effects on spatial frequency selectivity. **E, F.** This example shows TMS-induced facilitation in spatial frequency tuning run.

Author Manuscript

Author Manuscript

Author Manuscript

Author Manuscript

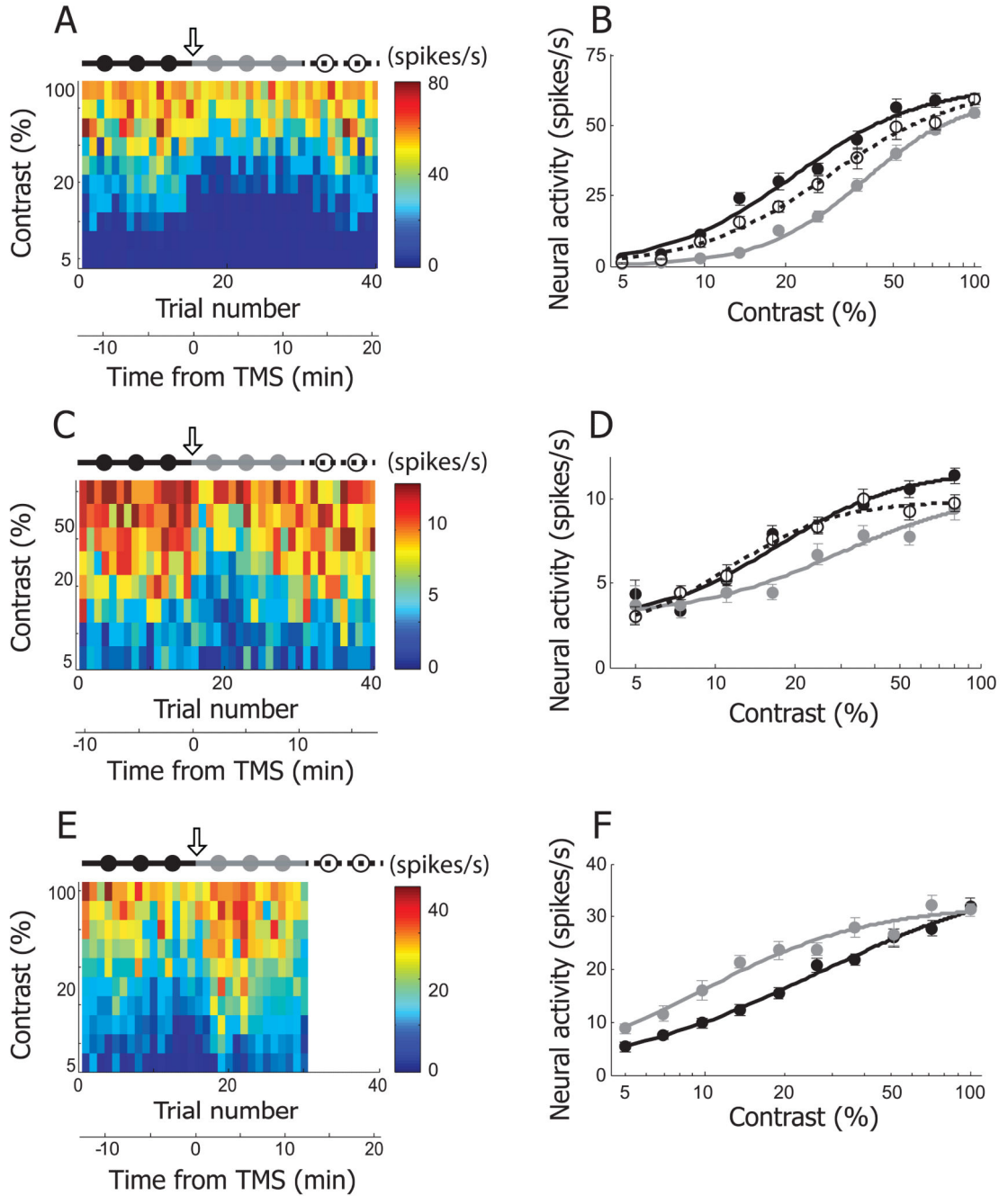
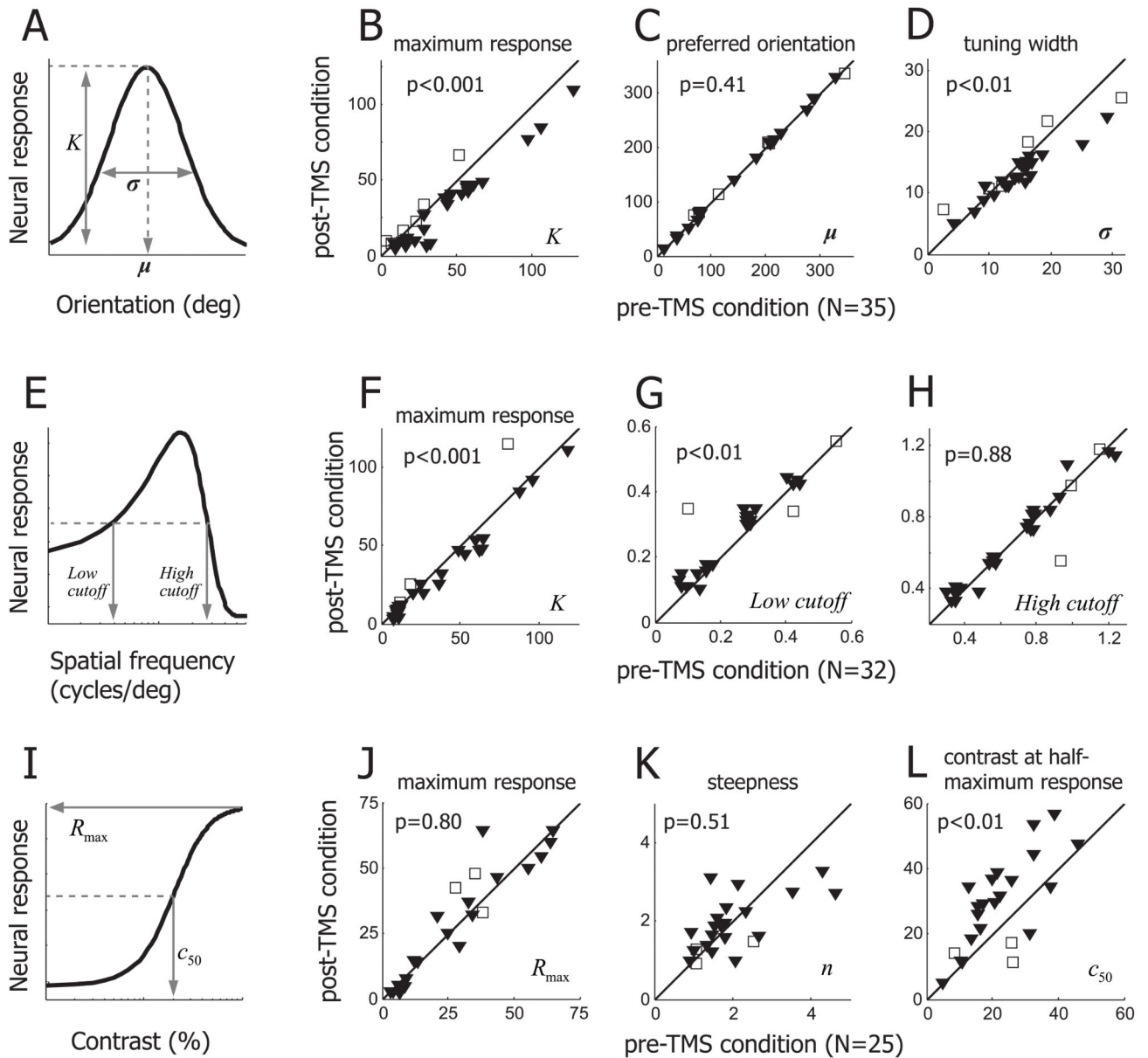


Figure 4.

Three examples showing TMS effects on contrast selectivity. **A.** In this example cell, neural responses for 10 different contrast values (5~100%, evenly distributed in logarithmic scale) were recorded in 40 trials. The plotting conventions are the same as in Figure 2A. 4Hz rTMS (downward arrow) was applied just before the 16th trial. The total 40 trials are divided into three groups to create tuning functions in pre-TMS (1~15th trials, black filled circles and line), post-TMS (16~30th trials, gray filled circles and line), and recovery (31~40th trials, open circles and dotted line) conditions. **B.** Contrast tuning curves of pre-TMS, post-

TMS and recovery conditions were created from the cell depicted in (A). The curves are

fitted with the Naka-Rushton function, $R(c) = \frac{R_{max}C^n}{C^n + C_{50}^n} + R_0$. The area under gray curve (post-TMS condition) is smaller than those of the other two curves. Note that despite of TMS-induced suppression, response magnitude at the lowest (5%) and highest (100%) contrast is comparable in pre- and post-TMS condition. More detailed analysis of TMS-effects on contrast selectivity will be dealt in Figure 5I~L. **C, D.** Another example cell showing TMS effects on contrast selectivity. **E, F.** This example shows TMS-induced facilitation in contrast tuning run. Neural response for recovery condition was not recorded, so the matrix in (A) is blank between 31st and 40th trials.

**Figure 5.**

Summary of TMS effects on response selectivity. **A, B, C, D.** TMS effects on orientation selectivity were tested in 35 cells. **(A)** Three parameters (K , μ , σ) representing the maximum neural response, preferred orientation, tuning width are taken from Gaussian fitting function. **(B)** Parameter K is compared between pre- and post-TMS conditions. Difference between two conditions is significant (Wilcoxon signed-rank test, $p < 0.001$). TMS-induced suppression and facilitation cases are indicated by filled triangles and open squares, respectively. **(C)** Parameter μ is compared between pre- and post-TMS conditions. Regardless of suppression or facilitation, the preferred orientation is not affected by TMS. **(D)** Parameter σ is compared between pre- and post-TMS conditions. TMS-induced suppression often makes orientation tuning sharper, and this change (reduced tuning width)

is statistically significant (Wilcoxon signed-rank test, $p < 0.01$). **E, F, G, H.** TMS effects on spatial frequency selectivity were tested in 32 single units. (E) Parameter K represents the maximum neural response. Low and high cutoff spatial frequencies were defined as the lower and higher spatial frequencies evoking the half-maximum neural response, respectively. (F) Parameter K is significantly decreased in post-TMS condition (Wilcoxon signed-rank test, $p < 0.001$). (G) Low cutoff spatial frequency is significantly higher in post-TMS than pre-TMS conditions (Wilcoxon signed-rank test, $p < 0.01$). (H) High cutoff spatial frequency is not significantly changed between pre- and post-TMS conditions. **I, J, K, L.** TMS effects on contrast selectivity were tested in 25 single units. (I) Three parameters (R_{\max} , n , c_{50}), taken from Naka-Rushton function, represent the saturated neural response, steepness of curve, stimulus contrast producing the half-maximum neural response, respectively. (J) Parameter R_{\max} is not significantly changed by TMS (Wilcoxon signed-rank test, $p = 0.80$). (K) Parameter n is compared between pre- and post-TMS conditions. (L) Parameter c_{50} is significantly increased in post-TMS condition (Wilcoxon signed-rank test, $p < 0.01$). Considering (J) and (L) together, results suggest that TMS effects on neural response are better explained by contrast-gain rather than response gain control.